16th World Conference on Earthquake Engineering, 16WCEE 2017

Santiago Chile, January 9th to 13th 2017

Paper N° 3679

Registration Code: S-L1464058431

A LONG-STROKE SEMI-ACTIVE MR DAMPER FOR BUILDING CONTROL USING TUNED MASSES

R. Zemp[(1)], J.C. de la Llera[(2)], J.L. Almazan[(3)], F. Weber[(4)]

[(1)] *Ph.D., National Research Center for Integrated Natural Disaster Management (CIGIDEN) CONICYT/FONDAP/15110017, School of Engineering, Pontificia Universidad Católica de Chile, renezemp@bluewin.ch*

[(2)] *Principal Investigator, National Research Center for Integrated Natural Disaster Management (CIGIDEN), CONICYT/FONDAP/15110017, School of Engineering, Pontificia Universidad Católica de Chile, jcllera@ing.puc.cl*

[(3)] *School of Engineering, Pontificia Universidad Católica de Chile*

[(4)] *Empa, Swiss Federal Laboratories for Materials Science and Technology*

Abstract

In this research the comprehensive development of a long-stroke MR-damper designed to control the earthquake performance of an existing 21-story reinforced concrete building in Santiago (Chile) by reacting on one of its tuned masses is presented. The ±1 m stroke MR-damper design is quite unique and considered the nominal response of the building equipped with two pendular masses of weight 160 tons each, and tuned to the fundamental mode of the structure. The real-scale long-stroke MR-damper was designed by our research team and manufactured in Chile. The MR-damper was tested using a special testing rig designed to study devices with long stroke at large deformation velocities. The rig was implemented in the dynamics and vibration control laboratory at Universidad Catolica de Chile. Both, the long-stroke MR-damper and the control algorithm were experimentally validated using a suite of periodic and seismic signals. For the building numerical simulations, the nominal MR-damper force-displacement constitutive relationship was replaced by the measured force-displacement response of the damper in order to validate the theoretical MR-damper model used. Such model was used in simulations to predict the performance of the TM-MR damper assembly in the design phase of the damper. Furthermore, a new real-time structural displacement sensor was developed with this application since conventional technology and methods to measure building displacement are inaccurate for a real-time displacement control as proposed with this application. The real-time building displacement sensor was validated using a scaled-down building prototype subjected to shaking table tests before an actual size sensor was implemented within a test building. All electronic components of the tuned-mass MR-damper assembly were tested with a shaking table and subjected to strong motion accelerations while the MR-damper was working in its active mode. It is concluded that the proposed tuned-mass MR-damper solution is technically feasible and may be advantageous in some real-life situations. The stage of development of the technology reached a point that enables commercial implementation in a real structure.

Keywords: Tuned mass MR damper; Real-Time Structural Measurement; Large scale MR damper; Shaking Table Test

1. Introduction

In recent years, magneto-rheological dampers (MRD) have gained recognition in the area of semi-active structural control. In an MRD, the fluid changes in milliseconds from a free flowing fluid state to a semi-solid one when exposed to a magnetic field. Thus, an MRD can control the damping force level of a tuned mass (TM) in an adaptive way with a small requirement of power. In numerical simulations, different semi-active control strategies of TMDs have been used [1]-[5], and an adaptive tuned mass magneto-rheological damper (TM-MR damper) controller for bridge vibration has been evaluated numerically and tested experimentally ([6], [7]). Also, a scaled proof-of-concept implementation of a TM-MR damper assembly on a real building is described in detail elsewhere [8]. In previous literature [9], the quasi-static Bingham fluid model is proposed for MR design purposes, which parameters depend only on the known geometry of the MRD and the magneto-rheological fluid (MRF) properties. This Bingham fluid model was previously extended [10]. In a technical-economical evaluation described elsewhere [11] the MRD solution with that of an alternative passive viscous damper (VD) for an equal value of a key performance index is compared. It is shown in this study that for equal performance, the TM-MRD solution could be about 40% cheaper than a VD implementation.

With a complete literature review it is shown so far no long-stroke MR damper developed and manufactured. Indeed, test results for small amplitudes are presented in a true-scale medium stroke annular orifice MR damper with similar capacity (300 kN), but much smaller stroke of ±28cm [12]. Additional experimental results of another true-scale mid-range stroke bypass MRD with capacity 400 kN and stroke ±47.5 cm are also available [13]. Test results for a small-scale medium-stroke length MRD with capacity 2.5 kN and stroke +60 cm are presented in reference [14]. More recently, test results of a large-capacity MRD with an external cylinder (600 kN, ±20 cm) are also presented in reference [15].

This research focuses in technological aspects of the development and implementation of a TM-MR damper assembly aimed to improve the earthquake performance of a 21-story office building located in Santiago, Chile. Previous to the design and testing of the TM-MR damper assembly, a large number of numerical simulations were developed to validate the vibration control strategy of the building. The building has a large plan aspect ratio of 3.4, and lateral-torsional coupling ([5], [8]). Based on simulations, a ±1m MRD with a nominal force capacity of 300 kN was designed and manufactured.

Real-time displacement measurements of structures are extensively discussed in the area of structural identification and health monitoring, but not as much in structural control. In available literature [16]-[18] alternative methods to measure building displacements in real-time are shown, but unfortunately these solutions are inadequate in this case due to the delay in these measurements, the feasibility to measure the required building motions, and the space limitations for measuring building displacements. The information required by the extended physical controller developed in this research [11] uses the displacement of the building at one location and the sign of the damper force. Hence, building displacements are measured using a new real-time structural measurement (RTSM) sensor developed and tested in this research [19]. Forces are obtained using a load-cell integrated to the damper chassis [11]. Furthermore, a low-cost fast response current driver for the long stroke magneto-rheological damper (MRD-L) coils was designed, manufactured, and tested [11]. These three technical aspects are essential in achieving a good control and performance of the MRD. Moreover, testing a MRD-L required a new testing rig to achieve full damper amplitudes and high damper velocities. The manufactured ±1 m stroke MRD-L and controller was extensively tested with cyclic periodic signals and seismic motions.

A critical aspect to be investigated in the control system is the lag between rise-time of the coil current and damper force. To evaluate the impact of variations in the force values, building simulations were performed by replacing into the structural model the nominal forces of the damper by the experimental values. Thus, the performance of the *quasi* pseudo-dynamic system was compared in this article with that obtained from simulations using the nominal behavior of the TM damper assembly. Finally, results of shaking table tests of all electronic components of the manufactured controller for the proposed TM-MRD solution are presented.

2. TM-MR damper assembly for building control

Shown in Figure 1 is a schematic representation of the developed TM-MR damper assembly proposed for building PA. The building is more flexible in the transversal Y-direction (T_{y1} = 2.68s and T_{x1} = 1.30s), and hence, the MRD will be connected to either of the TMs in the Y-direction—the west mass was chosen because the displacement is larger at this edge of the building. As shown in the Figure, the components of the TM-MR damper assembly are: (1) the two pendular TMs; (2) the long stroke MRD-L; (3) the new RTSM displacement sensor, which values u_y are used by the damper controller; (4) the load-cell measuring the damper force F in real time, also used by the damper controller; (5) the potentiometer measuring the relative displacement p_y between the TM and structure; (6) the data acquisition system (DAQ), which has two parts—DAQ 6.1 installed next to the MRD-L and DAQ 6.2 installed at the basement next to the RTSM sensor; (7) the industrial computer running the damper controller; (8) the current driver; (9) the voltage source feeding all sensors and electronic components of the current driver; (10) the power backup system (UPS); and (11) all the additional sensors used for monitoring the behavior of the TM-MR system and structure before, during, and after the earthquake. Red lines in Figure 1 represent data used by the real-time damper control; blue lines indicate the power supply of different components; and black lines indicate the flow of data acquired for monitoring purposes.

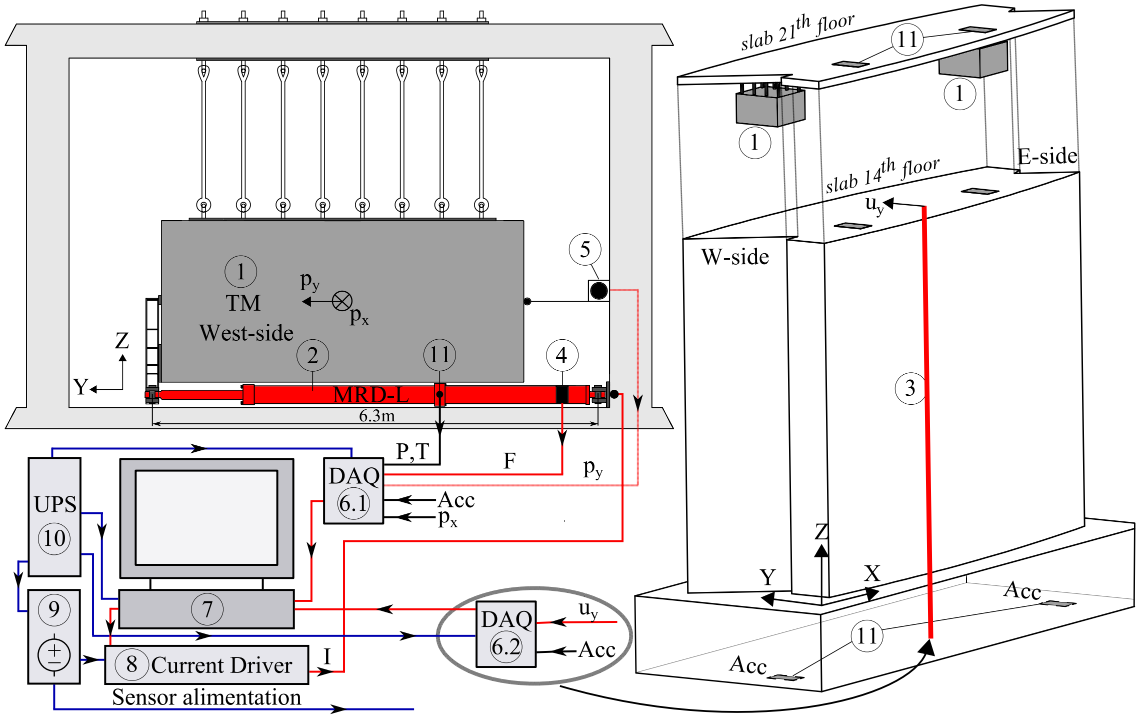

Figure 1 – Schematic view of building PA with the TM-MR damper assembly and operational data flows.

Some system components and functions not further explained in this article are: the specially for this application designed and manufactured current driver base on five 12V batteries with 7Ah each and with a PIC18F2550 microcontroller (8) [11], the integrated load cell (4), the signal p_y of the potentiometer (5), which is only used as a trigger to start or stop the action of the semi-active control—in this application the control is activated when the TM displacement exceeds 4 cm, and stops if that displacement is less than 4 cm for more than 10s; the industrial computer (7), which stores all the measured signals collected by the DAQ system (6)—in sleeping mode, the system is continuously sampling 60s of data at 100Hz and saving it into memory, and hence, for an earthquake the data collected includes 60s before the MRD-L control activates and 60s after the control disengages; other system variables obtained by additional sensors (11) that measure the internal pressure P and temperature T of the damper, the floor accelerations at different stories, and the displacement p_x of the TM in the X-direction.

3. Simulation results of the semi-active building control

Building PA is equipped with two pendular masses 160 tons each hanging from the roof building level. The TMs were designed to control earthquake induced vibrations mainly in the transverse building direction, Y, which nominal vibration period is T_{y1} = 2.68s. The total mass of the two TMs equals 1.19% of the modal mass associated with the first building mode. Additional detailed information of the building structure with TMs was presented earlier ([5], [8]). In reference [5] it is shown that the effectiveness of the TMDs in this building depends on the frequency content of the earthquake.

MR damping is used to improve the seismic performance of the building by acting on the TMs. The seismic performance of the TM-MR damper assembly is compared with that of a passive TM-viscous damper (VD) assembly. In simulations, 8 recorded ground motions of different Chilean earthquakes were used. The dynamic building model was assumed linear with 3 degrees of freedom (DOFs) per floor (X-, Y-, and θ-). The model was obtained by dynamically reducing the 3D building model with 153’850 DOFs to a reduced dynamic model of the structure with 20 Ritz-vectors. The pendular TMs were defined by 2 horizontal DOFs each considering large displacements. Internal damping ratio for the structure was constant and equal to 2.5%. More information about the building model with the TM-MR damper assembly is presented elsewhere [5].

Simulations considered two different structural cases: (a) the structure with nominal periods (T_{y1} = 2.68s); and (b) the structure with true measured periods (T_{y1} = 2.10s) obtained on the building by using micro-vibration tests at the end of the construction process. Detailed information obtained from this building identification is available in [8]. Due to cracking and inelastic behavior, structural periods increase during the earthquake. Thus the two structural cases represent lower and upper bounds of the periods of the building. In the case of nominal building periods, the TMs are tuned exactly to the first mode while for the case of measured periods, the TMs are out of tuning. Three different cases of the TM damper assembly were considered in simulations: (I) TMs without any supplemental damping; (II) TMs with available VDs in the Y-direction, with properties in agreement with those used in the real implementation, i.e., c = 56’900kg/m and α = 2, resulting in a total capacity of 650kN; and (III) TMs with MRDs in the Y-direction.

MRDs were modeled by the well-known *quasi* static Bingham model ([9], [10]), since more sophisticated dynamic models required experimental data in advance for calibration. To control the semi-active MRD-L, a new extended physical controller was developed in this research and discussed earlier [11]. This new controller uses a simple on-off control strategy that results in equal performance compared to other existing controllers, but has the advantage of implementation simplicity in a real building. Because the first nominal period in the X-direction of the building is 1.30s, no X-direction dampers were used since TMs are completely detuned in that direction.

Shown in Table 1 are the Peak and the Root Mean Square (RMS) displacement reductions in the building according to the simulation results. The reduction of earthquake displacement are all relative to the bare-structure case (without TMs) and the following cases: (Ia) building model with nominal periods and TMs without supplemental damping; (Ib) building model with true periods and TMs without supplemental damping; (IIa) building model with nominal periods and TMs with VDs in the Y-direction; (IIb) building model with true periods and TMs with VDs in the Y-direction; (IIIa) building model with nominal periods and TMs with MRDs in the Y-direction; and (IIIb) building model with true periods and TMs with MRDs in the Y-direction. The reduction in the Y-direction given in this Table corresponds to the relative displacement between the 14th floor and the base. This displacement is the one used by the real-time controller and corresponds to the building displacement excluded the participation of the second mode as explained later.

It is apparent from the results shown in this Table that the best building performance is obtained with the TM-MR damper assembly. Also shown is the very sensitive reduction in response of TMs without dampers. Indeed, peak building displacements are significantly reduced in this case for some earthquake records, but increased for other records. Viscous dampers improve the performance of the bare TMs, but the TM-MR solution works better especially if the TMs are detuned. Reduction values for the TM-MR damper assembly depend on the earthquake and may reach 51%. Mean values of Peak reduction are between 14% and 17%, and mean RMS values between 24% and 35%. To better assess the relevance of these numbers please note that the total mass of the two TMs represents only 0.47% of the total building mass including all 6 basements, and 0.95% without basements. Moreover, the total capacity of the two MRDs represents 0.09% of the total building weight. In reference [5] more results of the simulation of this building with a TM-MR damper assembly are available. A cost comparison of the proposed TM-MR solution and the VD case is shown in [11]. It turns out that for equal performance, the MRD solution is about 40% cheaper than the VD solution,

Table 1 – Y-direction reduction in Peak and (RMS) displacements for the 14th floor relative to the base (%).

Case		Chilean earthquake records								
		S. Felipe (1985)	Melipilla (1985)	Llolleo (1985)	S. Isidro (1985)	Pichilemu (1985)	Antumapu (2010)	San Pedro (2010)	C. Roble (2010)	Mean.
PGA (g)		0.31	0.69	0.74	0.81	0.28	0.27	0.66	0.19	
TM	Ia	10 (0)	40 (24)	-22 (-18)	6 (18)	-9 (-12)	0 (6)	36 (27)	-22 (-22)	5 (3)
	Ib	-14 (-5)	3 (-10)	-4 (-12)	11 (7)	-1 (6)	-7 (-7)	-4 (-2)	6 (1)	-1 (-3)
TM & VD	IIa	10 (25)	21 (37)	-4 (21)	20 (39)	-5 (10)	16 (33)	36 (46)	1 (15)	12 (28)
	IIb	-1 (7)	7 (8)	5 (7)	6 (18)	16 (14)	2 (3)	2 (11)	10 (9)	6 (9)
TM & MRD	IIIa	16 (34)	25 (44)	-5 (25)	25 (41)	3 (23)	25 (38)	40 (51)	8 (25)	17 (35)
	IIIb	10 (21)	18 (27)	9 (16)	12 (37)	28 (30)	4 (16)	11 (26)	19 (20)	14 (24)

4. Real-time structural measurement (RTSM) system

As presented in Figure 1, the developed controller of the TM-MR damper assembly needs the building displacement and the sign of the MRD-L force [11]. However, measuring floor displacements in real-time is not straight forward. If displacement were obtained by double integration of the acceleration signal, the signal needs to be high-pass filtered in real-time before integration, leading to a delay in time which would significantly decrease the performance of the controller. Consequently, different solutions were evaluated before coming up with the proposed RTSM sensor [19]. Shown in Figure 2(a) is a schematic view of the RTSM sensor proposed to measure building displacements. Conceptually, a string is attached between the basement and the floor where relative displacement needs to be measured. As the building deforms, the angle φ is measured in real-time and the floor displacement computed using the length of the string. For building PA, the string is attached at the basement and the 14th floor slab (Figure 1). This level corresponds to a node of the second mode, and the contribution of this mode to the displacement is negligible (Figure 2(a)). Because the TM is tuned to the fundamental mode, the performance of the TM itself is optimal if excited in that mode. Therefore, it was intuitive to try out in simulations of the building, the case with a control signal that eliminates the participation of the second mode in the displacement. Many simulations support this idea that leads to the best building performance. Using instead the roof displacement, it leads to a slightly worse performance. Moreover, in a real implementation this has another disadvantage: the length of the displacement sensor would be longer and more vibration noise would be introduced into the signal.

Shaking table tests of a scaled proof-of-concept sensor were performed at *Empa*, Switzerland. Shown in Figure 2(b) is a photo of the test setup; different earthquake records were applied by the actuator to the 5-story building model and the displacements was measured by the string sensor. Also shown in Figure 2(c) is a comparison between the target and measured displacement for the Melipilla record (Chile, 1985). While the blue line represents the displacement measured by the RTSM sensor, the red line represents the target displacement measured by two laser sensors at the base and roof of the structure. It is observed that the RTSM sensor tracks the target signal well and the sensor may be used to track the building displacement for real-time structural control.

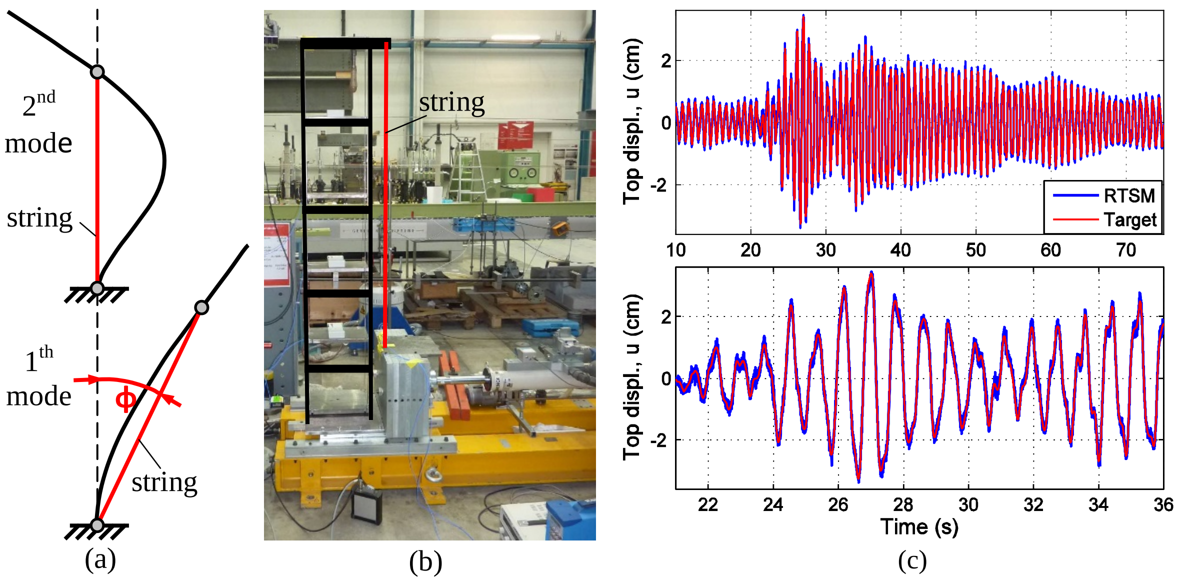

Figure 2 – Deployment of the RTSM sensor: (a) sketch of string attached to the deforming structure; (b) reduced scaled shaking table tests; and (c) comparison of RTSM sensor results for shaking table test.

However, during the earthquake the taut string will vibrate and this vibration may generate undesirable noise in the displacement signal. The higher the modal eigen-frequencies of the string, the smaller the noise. Recall that the undamped eigen-frequencies f_n of a taut string are:

$$f_n = \frac{n}{2L}\sqrt{\frac{\sigma}{\mu}} \qquad n = 1,2,3.... \qquad (1)$$

where L is the string length; μ is the mass per unit length; and σ is the tension in the string. For a given length of string, the resulting frequencies increases as μ decreases and the tension increases. Therefore, an ideal string material is a carbon fiber (FRP) since it is light and stiff. A 57.3m long string sensor was designed and fabricated using FRP, but previous to installation, the anchorage system of the FRP-lamella was thoroughly tested. Additionally the displacement sensor was numerically simulated to study the effect of vibration noise in its measurements. More information on these topics can be found elsewhere [11].

5. Seismic tests on long stroke MRD-L

The comprehensive testing program on the MRD-L included a total of 170 cyclic and seismic tests. Results of scaled seismic tests are presented herein, and tests with constant current are discussed elsewhere [10]. The MTS actuator used has a stroke of ±0.5m, a nominal force capacity of 1000kN and peak velocities of about 16cm/s. To test the MRD-L at full stroke, and to increase the piston velocity, a mechanical displacement and velocity amplifier was added to the existing test rig (Figure 3). The MRD-L (1) was placed on top of the rig, and the piston of the damper was connected to the top of the rotating beam (2) facing the damper. The rotation of the beam was controlled by the actuator (3), and the axis of rotation of the front lever beam was vertically adjusted (4) to modify the kinematic amplification. The optimal axis of rotation is a trade-off between damper force and velocity. In the configuration shown in the Figure, the kinematic amplification is 1:2.33 and most of the tests in constant-current and controlled-mode were performed in this configuration. The real actuator delivers about 700kN for a velocity of 19cm/s. So, the maximum damper velocity obtained in this configuration is 2.33 * 19cm/s = 45cm/s at a maximum possible damper force of 700kN / 2.33 = 300kN. For the zero-current damper tests with smaller damper forces, the rotation axis was moved down 3 slots to reach a kinematic amplification of 1:5.67, and the peak velocity achieved with the new setup was 100cm/s.

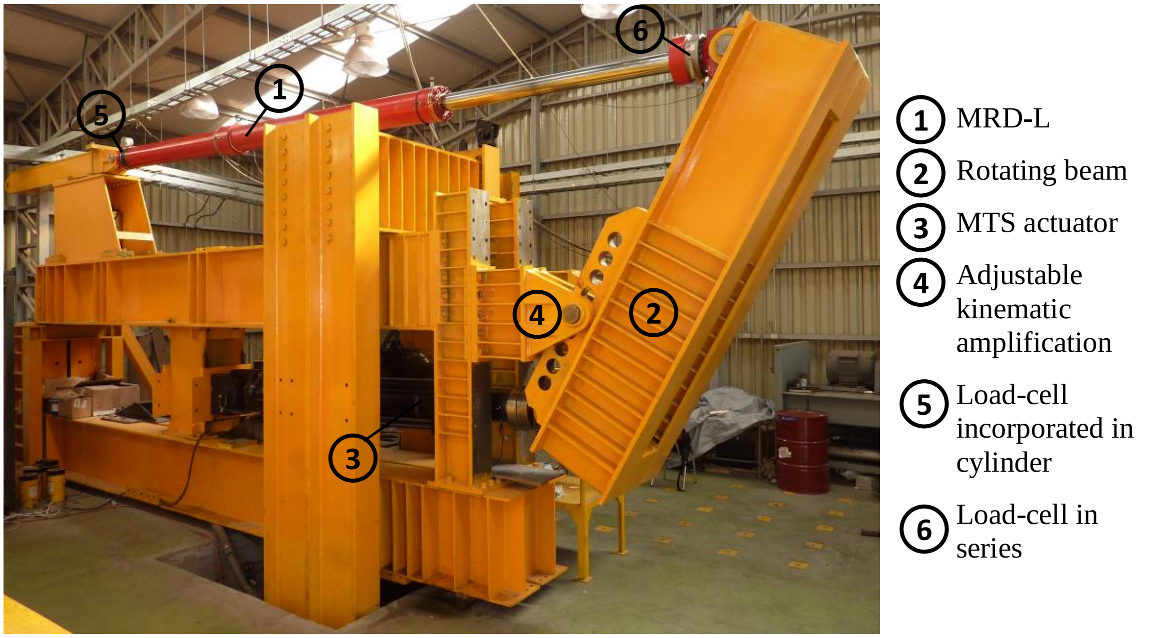

Figure 3 – Photo of modified laboratory test rig to run MRD-L tests at large earthquake velocities.

For seismic tests, the axial input signal of the damper displacement was obtained from off-line simulations of the building PA with the TM-MR damper assembly—a hybrid real-time testing would have been ideal, but with the current experimental setting it was not possible. During an earthquake, maximum piston velocities range from 100cm/s up to 350cm/s, depending on the earthquake record. Even with the kinematic amplifier, the latter velocities could not be reached with this setup. Therefore, the axial motion of the damper needed to be scaled down somehow. Tests with smaller velocities than real imply smaller damper forces in the zero-current damper tests, but such forces in the constant-current and controlled-mode do not change significantly as a result of reduced velocities. To achieve the velocity reduction needed, records were scaled in two different ways: (i) the displacement signals of the set of 8 seismic motions were scaled down by a factor; and (ii) the time of the 8 tests was stretched to reduce velocities while preserving the real damper displacements. Applied displacement reductions and time stretching factors were in the range 1.5 to 8; these values depend on the earthquake record and whether the damper is tested in its constant-current and controlled-mode or in the zero-current mode. By using these two sets, many experimental aspects could be adequately evaluated, such as the force-velocity and force-displacement constitutive relationship of the MRD-L, all functional aspects of the MRD-L controller, and important aspects related to the energy dissipation capacity of the damper.

Shown in Figure 4 are the test results of the force-displacement and force-velocity constitutive relationship obtained by a controlled MRD-L test, in which the coil current intensity of the damper is controlled in the test. The displacement input for the damper in this case corresponds to the building response for the Llolleo record (Chile, 1985). It is seen that the controller changes force between the peak-current and the zero-current force levels. Maximum peak-current force is 320kN, and maximum zero-current force level is about 40kN, which results in a dynamic range of 8, approximately. Shown in Figure 4 is the damper force in constant-current mode (other test with constant current superposed with dashed red line) is U-shaped and increases as the amplitude of the cycles increase. This effect was denoted as a force drop-off behavior and is discussed in detail elsewhere [10].

In some of the tests, the control system operated completely independent from the electrical network. Also, by adding all the 170 cyclic and seismic tests, more than 220MJ of energy were dissipated. This is about 39 times the energy needed during a large earthquake. A peak internal fluid pressure of 690 bars was measured and no damage or failure was observed in the damper seals. With this extensive testing program, the short-term functionality of the proof-of-concept MRD-L and its control were validated for a real building implementation. By using 36 tests in zero-current-mode it was shown that the baseline damping level of the TM-MR damper assembly is between 8 to 12%, which is deemed adequate. Consequently, the MRD-L works as a passive damper in the worst case scenario if the controller fails for any unlikely reason. In such a case, the extra benefit of the semi-active control would be lost, but the building would remain safe. More results of the extensive testing program are found in references [10] and [11].

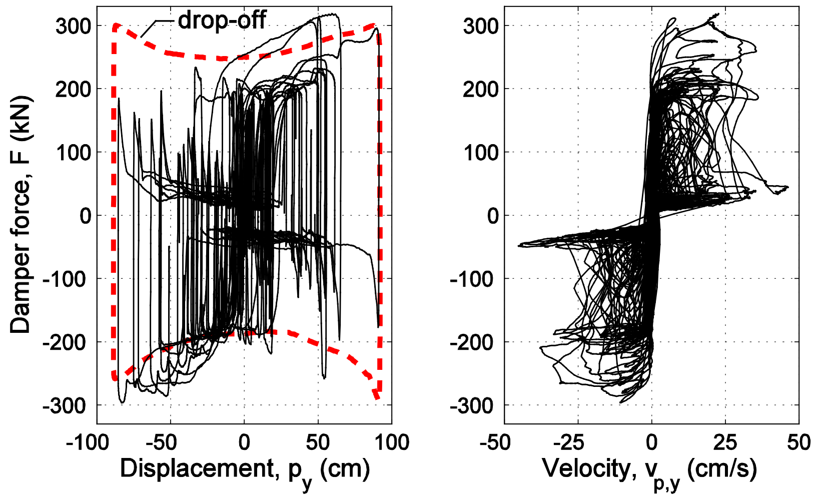

Figure 4 – MRD-L force-displacement and force-velocity constitutive relationships for the Llolleo record (Chile, 1985) with MRD-L in controlled mode.

6. Simulation of the building performance using the measured MRD-L behavior

The quasi-static well-known Bingham fluid model [9] was used in simulations to evaluate building performance and MR damper design before manufacturing. This model of the damper was selected because it requires no a-priori experimental damper data at the design stage of the MRD-L. In the Bingham model, the constant-current and zero-current damper forces are modeled only using the MRD geometry, the piston velocity, the passive fluid viscosity, and the shear strength of the MRF in constant-current-mode. This contrasts with essentially all dynamic MRD models available in the literature (e.g. [12], [20] and [21]) that require a parameter calibration and/or model training. One disadvantage, however, of the Bingham fluid model is that the force-displacement and force-velocity constitutive behavior is not always accurately represented. Larger discrepancies between the model and tests are observed as the piston velocity changes sign, as the damper state shifts from zero-current to the peak-current state and vice versa, and with the force drop-off behavior that cannot be accounted for by the Bingham model.

The question is how good the prediction of the damper performance is by using this simple model. To get an answer, the so-called *quasi* pseudo-dynamic tests are performed without considering the coupling effects of the building and MRD-L. Real pseudo dynamic tests which would consider this coupling effect were not possible for the MRD-L, but were performed for a scaled MRD as presented elsewhere [8]. So *quasi* pseudo-dynamic simulations of the building with the MRD-L were performed to verify the displacement reduction values shown in Table 1 using the TM-MR damper assembly and the measured MRD-L behavior. These simulations included three steps. First, seismic simulations of the building with the TM-MR damper assembly were carried out using the nominal Bingham fluid model for the damper ([9], [10]). Secondly, with the nominal damper response, semi-actively controlled seismic tests were performed on the damper at the laboratory. These tests provide the force in the MRD-L corresponding to the imposed displacement that results from the nominal seismic response of the building. Piston velocity, as the first derivative of the displacement signal, is applied implicitly when applying the displacement to the damper. Since the actuator cannot track the command displacement signal perfectly well in reality, the resulting velocity has an error, which is not significant for this application. Thirdly, seismic simulations were repeated on the building but using the measured force-displacement relationship obtained from the controlled damper test. These simulations are denoted as *quasi* pseudo-dynamic tests— the prefix *quasi* is used because there is no real-time interaction or coupling between the simulation and test. Thus, the TM-MR damper assembly is replaced in the building model after ending the damper test as a pre-defined force that results from two sources: the measured MRD-L force and the reaction force of the TM on the structure. The coupled effect between TM, MRD-L, and the structure may only be obtained by true hybrid simulations. Sixteen *quasi* pseudo-dynamic tests were performed and results are presented next.

Shown in Figure 5 is a typical comparison between the seismic displacement of the 14th floor for three models of the building subjected to the San Isidro earthquake record (Chile, 1985). These models are: (i) the bare structure without TMs; (ii) the structure with a nominal model of the TM-MR damper assembly; and (iii) the structure with the TMs and the measured MRD-L response *(quasi* pseudo-dynamic test). The most relevant observation is that there is no significant difference in the building displacements obtained using the simulation with the Bingham damper model and the simulation using the measured MRD-L force-displacement constitutive relationship.

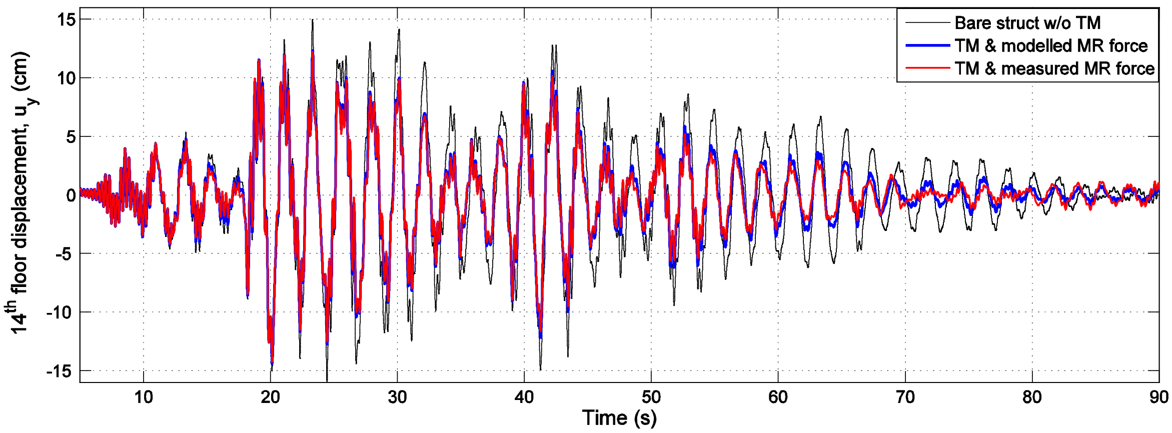

Figure 5 – Comparison of the 14th floor roof displacement history of the building subjected to the San Isidro record (Chile, 1985) using the nominal (Bingham model) and measured MRD-L behavior.

Summarized in Table 2 are the peak and RMS displacement reductions at the 14th floor with respect to the bare structure subjected to the 8 seismic records. Four different models are considered in this comparison, which are denoted with letters A-D. In all models, the building was represented using the measured building periods. The west and east TMs are equipped with one MRD-L as developed and one commercial VD, respectively. Such is the case because it corresponds to the planned solution for the final building implementation. Results for cases A and B correspond to the displacement reductions obtained from the nominal model of the TM-MR damper assembly. Case A considers the basic physical controller, and Case B, the extended physical controller described earlier [11]. Displacement reductions for cases C and D are obtained using the measured MRD-L force-displacement constitutive relationship obtained experimentally and using the extended physical controller. For Case C, the MRD-L force is obtained using real-time and scaled displacement tests, and for Case D the force in the damper is obtained by time stretching and real displacements. In simulations with the simple Bingham model, both controllers have similar performance (Case A compared to Case B). This is different for a real building implementation because the Bingham model does not consider the slow force increase effect of the damper, which reduces the performance of the basic physical controller—this was the reason to extend the physical controller. Comparing results from cases C and D with those of Case B, no significant change in building performance is observed between simulations using the nominal and measured MRD-L force-displacement constitutive relationship. This observation is important because it justifies the use of the simple Bingham model to predict the damper performance for building design purposes, prior to send the device to fabrication. Average displacement reductions turn out to be very stable between models reaching 10% or 11% and 19% for peak and RMS responses, respectively.

Table 2 – Peak and (RMS) 14th floor displacement reductions (%) in the Y-direction using measured building periods and TMs, one with an MRD-L and the other with a VD.

Case	Chilean earthquake records								
	S. Felipe (1985)	Melipilla (1985)	Llolleo (1985)	S. Isidro (1985)	Pichilemu (1985)	Antumapu (2010)	San Pedro (2010)	C. Roble (2010)	Mean
A	5 (16)	14 (21)	7 (12)	10 (32)	27 (26)	2 (12)	8 (20)	15 (15)	11 (19)
B	7 (17)	11 (19)	7 (13)	9 (28)	23 (23)	2 (11)	7 (19)	15 (14)	10 (18)
C	6 (16)	12 (21)	7 (13)	11 (32)	24 (23)	0 (12)	9 (20)	16 (15)	11 (19)
D	7 (16)	11 (20)	7 (12)	10 (30)	25 (25)	1 (12)	7 (19)	15 (16)	10 (19)

Case B in Table 2 represents the same structural model and control case as presented in Case IIIb of Table 1. However, as opposed to Case IIIb, where both TMs are equipped with an MRD, in Case B one TM is equipped with an MRD and the other with a VD. Comparing these two cases it is shown that the building equipped with two MRDs has in general a better performance than the building with one TM-MR and one TM-VD assembly. Such improvement is in this case (and using measured building periods) in average 4% and 6% for peak and RMS displacement reductions, respectively. Additionally, this result shows that it is perfectly possible to have a passive and a semi-active damper running in parallel in the same building.

7. Shaking Table Test of electronic components of MRD control

During a strong motion earthquake, the electronic components of the MRD controller shown in Figure 1 to control the MRD are exposed to high levels of accelerations. To evaluate the performance of the MRD controller installed on the top floor of building PA in real earthquake conditions, all these electronic components were tested on a shaking table with six degrees of freedom. The shaking table has a maximum stroke of 30cm in the horizontal direction and 18cm in the vertical direction. The motion applied to the electronic components in these shaking table tests were the simulated building motions at the point where the electronic components were supposed to be installed. These motions correspond to the 8 earthquake records used previously in Sections 3 and 6. Due to the stroke limitation of the shaking table it was not possible to apply real earthquake displacements. Therefore, the input motions for the shaking table were scaled to reduce displacements while maintaining accelerations.

The measured peak accelerations applied during these tests are shown in Table 3 for the different earthquake inputs. Maximum acceleration reached levels up to 0.97g in the X- direction, 1.75g in the Y-direction and 0.78g in the Z-direction. During these tests, the controller, including the DAQ, the industrial computer, the current driver, the voltage source, and the UPS were in active mode, i.e. with controlled coil current in the MRD. In all these tests, no failure of any of these components or degradation in performance under the applied accelerations could be observed. This test proves the correct functionality of the MRD controller under real acceleration conditions during an earthquake.

Table 3 – Measured peak acceleration (g) applied to the electronic components of the MRD controller during shaking table tests and different earthquake records.

Direction	Chilean earthquake records							
	S. Felipe (1985)	Melipilla (1985)	Llolleo (1985)	S. Isidro (1985)	Pichilemu (1985)	Antumapu (2010)	San Pedro (2010)	C. Roble (2010)
X	0.41	0.87	0.97	0.88	0.76	0.85	0.75	0.70
Y	1.17	1.41	1.75	1.75	1.21	1.23	1.13	1.19
Z	0.41	0.66	0.78	0.53	0.54	0.58	0.60	0.54

8. Conclusions

An MRD-L solution that includes a long-stroke damper, a controller, and a data acquisition system to control in real-time the earthquake performance of a free-plan 21-story building equipped with two TMs at the roof is shown in this study. It is concluded that the solution is technically and economically feasible. All mechanic and electronic components of the system were satisfactory tested using analytical models and experimental tests. In this particular application, the TM-MR damper assembly generates a better performance by about 9% relative to a solution using viscous dampers.

It is shown by numerical simulations on the building equipped with the TM-MR damper assembly and subjected to 8 Chilean earthquake records that peak and RMS displacement reductions relative to the response of the bare structure are between 14% and 35%. These values represent significant reductions in light of the small masses used for the TMs, which reach 1.19% of the modal mass of the first building mode. A real-case cost analysis was performed and it is shown that an implementation with MRDs to achieve equal performance would be about 40% cheaper relative to the viscous damper case.

A new real-time structural measurement (RTSM) system was proposed. The technology provides a reliable displacement signal for real-time control of a long-stroke MR damper. The sensor used was first validated using a series of shaking table tests with a scaled structure. Tests were run later on a real-scale prototype installed on a test-bed structure. Although beyond the scope of this research, this low-cost sensor could be very effective in other areas such as health monitoring.

A large set of experimental tests were performed on the built MRD-L. In spite of the total of 220MJ dissipated energy in all 170 tests, no damage or local failures of the damper seals were observed. It is concluded from seismic tests that the the MR damper as well as the developed controller operates properly.

Numerical simulations of the building were performed with the measured force-displacement behavior of the MRD-L rather than the nominal Bingham fluid model used previously in the literature. Results with the measured behavior are similar to the ones obtained with the nominal Bingham fluid model, and it is concluded that the control strategy used is robust. Thus, the Bingham fluid model may be used in simulating the MR damper behavior at least for design purposes of the building structure. This is important since this model does not require a priori knowledge of damper test data, which is very convenient in the design of a structure with a TM-MR damper assembly. As far as the authors know, this is the first attempt to legitimize the use of the simple Bingham model in simulations of a real building with a TM-MR damper assembly. Real pseudo-dynamic tests should be performed in the future to confirm this statement.

Finally, shaking table tests were performed on the electronic components of the system to prove their functionality during a strong motion earthquake and real acceleration conditions. Based on the results of these tests, all components worked properly and were validated for a real implementation.

9. Acknowledgements

The authors gratefully acknowledge the support of Pontificia Universidad Católica de Chile, and the Swiss Federal Laboratories for Materials Science and Technology, EMPA in Switzerland. This research has been sponsored by different research grants, Fondef Grant D07I1006, Corfo Grant 11IDL210806, Mecesup PUC 0710, Conicyt Grant 57090131, Fondecyt Grant 1110377, and Fondap Grant 15110017 and FONDECYT Grant #1141187. The authors are grateful for this continuous research support and that of the companies Lord Corporation and BASF for providing the MR fluids and their technical support; Revesol Inc. and the manufacturing team; VULCO Inc. for sponsoring the extension of the test machine; Sika for providing the FRP lamella; National Instruments for the help in the implementation of the controller; Hallite for the help with the damper sealing concept; SIRVE Inc. and Nüyün_tek and its teams for the technical support. Special thanks to Ch. Kieburg (BASF), D. Hodgson (Lord), M. Cerić and T. Berset (Sika), L. Elias and R, Riquelme (National Instruments), D. Meyerhoff (Hallite), H. A. Holtkamp and his team (Disynet), G. Schwegler (StressHead), and W. Zahlten (Bergische Universität Wuppertal), and the PUC professors R. Rodríguez, J. L. Almazán, P. Irarrázaval, and J. Dixon for their invaluable technical advises.

10.References

[1] Setareh M (2001): Application of semi-active tuned mass dampers to base-excited systems. *Earthquake Eng. & Struct. Dyn.,* **30** 449-62 DOI 10.1002/eqe.19.

[2] Runlin Y, Xiyuan Z, Xihui L (2002): Seismic structural control using semi-active tuned mass dampers. *Earthquake Eng. & Eng. Vib.,* **1** 111-18 DOI 10.1007/s11803-002-0014-0.

[3] Ji HR, Moon YJ, Kim CH, Lee IW (2005): Structural vibration control using semiactive tuned mass damper. *The 18th KKCNN Symposium on Civil Engineering—KAIST6,* Taiwan.

[4] Esteki K, Bagchi A, Sedaghati R (2011): Semi-Active Tuned Mass Damper for Seismic Applications. *Int. Workshop Smart Materials, Structures & NDT in Aerospace,* Canada.

[5] Zemp R, de la Llera JC, Almazán JL (2011): Tall building vibration control using a TM-MR damper assembly. *Earthquake Eng. & Struct. Dyn*., **40** 339-54 DOI 10.1002/eqe.1033.

[6] Weber F, Boston C, Maslanka M (2011): An adaptive tuned mass damper based on the emulation of positive and negative stiffness with an MR damper. *Smart Materials and Structures,* **20** DOI 10.1088/0964-1726/20/1/015012.

[7] Weber F, Maslanka M (2012): Frequency and damping adaptation of a TMD with controlled MR damper. *Smart Materials Structures,* **21** DOI 10.1088/0964-1726/21/5/055011.

[8] Zemp R, de la Llera JC, Roschke P (2011): Tall building vibration control using a TM-MR damper assembly: experimental results and implementation. *Earthquake Eng. & Struct. Dyn.,* **40** 257-71 DOI 10.1002/eqe.1021.

[9] Yang G (2001): Large-scale magnetorheological fluid damper for vibration mitigation: modeling, testing and control. *PhD. Dissertation,* University of Notre Dame, IN.

[10] Zemp R, de la Llera JC, Weber F (2014): Experimental analysis of a large capacity MR dampers with short- and long-stroke. *Smart Materials and Structures,* **23** 125028.

[11] Zemp R, de la Llera J C, Saldias H, Weber F (2016): Development of a long-stroke MR damper for a building with tuned masses. *Smart Materials and Structures,* (submitted for publication).

[12] Chae Y, Ricles JM, Richard Sause R (2012): Modeling of a large-scale magneto-rheological damper for seismic hazard mitigation. Part I: Passive mode. *Earthquake Eng. Struct. Dyn,*. DOI 10.1002/eqe.2237.

[13] Fujitani H, Sodeyama H, Tomura T, Hiwatashi T, Shiozaki Y, Hata K, Sunakoda K, Morishita S, Soda S (2003): Development of 400kN magnetorheological damper for a real base-isolated building. *Proc. of SPIE,* **5052** 265-76 DOI 10.1117/12.483810.

[14] Hongsheng H, Jiong W, Suxiang Q and Xuezheng J 2009 Test Modeling and Parameter Identification of a Gun Magnetorheological Recoil Damper *Proc. of IEEE International Conf. on Mechatronics and Automation* Changchun China 3431-3436 DOI 10.1109/ICMA.2009.5246327

[15] Sternberg A, Zemp R, de la Llera JC (2014): Multiphysics behavior of a magneto-rheological damper and experimental validation. *Engineering Structures,* **69** 194-205.

[16] Kijewski-Correa T, Kochly M (2007): Monitoring the wind-induced response of tall buildings: GPS performance and the issue of multipath effects. *J. of Wind Engineering and Industrial Aerodynamics,* **95** 1176–98.

[17] Matsuya I, Tomishi R, Sato M et al (2011): Development of Lateral Displacement Sensor for Real-Time Detection of Structural Damage. *IEEJ Transactions on Electrical and Electronic Engineering,* **6** 266–72 DOI 10.1002/tee.20654.

[18] Lee JH, Ho HN, Shinozuka M, Lee JJ (2012): An advanced vision-based system for real-time displacement measurement of high-rise buildings. *Smart Materials and Structures,* **21** (12) DOI 10.1088/0964-1726/21/12/125019.

[19] Zemp R, de la Llera JC (2015): Real-time structural measurement (RTSM) for control devices. *Patent,* US2015/0247754A1.

[20] Chae Y, Ricles JM, Sause R (2012): Modeling of a large-scale magneto-rheological damper for seismic hazard mitigation. Part II: Semi-active mode. *Earthquake Eng. & Struct. Dyn.*, DOI 10.1002/eqe.2236.

[21] Schurter KC, Roschke PN (2000): Fuzzy modeling of a magnetorheological damper using ANFIS. Proc. of the IEEE Fuzzy Conf., San Antonio TX 1 122–27.